Proceedings of the 1999 IEEE
International Conference on Robotics & Automation
Detroit, Michigan • May 1999

A SENSOR GUIDED AUTONOMOUS PARKING SYSTEM FOR NONHOLONOMIC MOBILE ROBOTS

K. Jiang School of Manufacturing & Mechanical Engineering, The University of Birmingham B15 2TT UK
and L. D. Seneviratne Department of Mechanical Engineering, King's College London WC2R 2LS UK

Abstract: An automated parallel parking strategy for a car-like mobile robot is presented. The study considers general cases of parallel parking for a rectangular robot within a rectangular space. The system works in three phases. In scanning phase, the parking environment is detected by ultrasonic sensors mounted on the robot and a parking position and manoeuvring path is produced if the space is sufficient. Then in the positioning phase, the robot reverses to the edge of the parking space avoiding potential collisions. Finally in manoeuvring phase, the robot moves to the parking position in the parking space in a unified pattern, which may requires backward and forward manoeuvres depending on the dimensions of the parking space. Motion characteristics of this kind of robots are modeled, taking into account the non-holonomic constraints acting on the car-like robot. On the basis of the characteristics, a collision-free path is planned in reference to the surroundings. The strategy has been integrated into an automated parking system, and implemented in a modified B12 mobile robot, showing capable of safe parking in tight situations. The system is developed for an automated parking device to help vehicle drivers. It also shows the potential to be integrated into automobiles.

1. INTRODUCTION

A study of the parallel parking problem for a car-like mobile robot is presented. This study is a part of a research project in the development of an automated car-parking system. A car-like robot is used to simulate a four-wheel vehicle. The robot has the same features as a four-wheel vehicle, such as a rectangular rigid body with two degrees of freedom (dof), which are a linear dof for forward and backward movement and a rotational dof for changing orientation. Generally, the robot is subjected to two non-holonomic constraints, which limit the steering angle, thus path curvature, and force the robot to move towards tangential directions of the path.

The research in car-parking problem is derived from the study of general motion planning for robots. In the past few decades, many algorithms have been developed in general robot motion planning. However, in the development of a parking guiding device, it is found difficult to apply those algorithms into car-parking cases for producing a result in real-time.

Lafferiere and Sussmann[1] presented the first general planner for car-like robots based on a constructive proof of controllability. Murray and Sastry [2] showed how to solve the problem for some canonical systems. However, both papers do not address obstacle avoidance, as pointed out by Sussmann and Liu [3]. Jacobs, Laumond and Taix [4] improved the situation by presenting a complete planner for mobile robots and showed that its strategy can be generalized. The algorithm consists of three stages: (a) plan a path π for the corresponding holonomic system; (b) subdivide π until all endpoints can be linked by a minimal length collision-free feasible path; and (c) run an "optimization" routine to reduce the length of the path [5]. An example of car parking is given, running in time 3.7 seconds on a SUN Sparc 2 workstation. This algorithm has been further tested [6] for a car-like mobile robot moving in complex environments consisting of a number of polygonal obstacles. In one of the given examples of five obstacles, the processing time on a SUN Sparc 2 workstation is 38 seconds.

In recent years, interest in car parking problems has increased. Paromtchikand and Laugier [7] presented an approach to parallel parking for a nonholonomic vehicle. In the approach a parking space is scanned before the vehicle reverses into the parking bay. The vehicle follows a sinusoidal path in backward motion, while the forward motion is along a straight line without sideways displacement. As no appropriate relationships are found for predicting collisions during parking manoeuvres, the approach employed a lookup table, built in offline, to estimate a collision-free start position for entering the parking space and estimate the travelling times for manoeuvres within the parking space. The possible collision during reverse between the vehicle and the longitudinal boundary of the parking space is not discussed. Some other studies are concerned with constructing controllers using a variety of newly emerged techniques, such as neural networks and fuzzy control. Only a few papers discuss the case of building an automatic parking system for a car-like vehicle. Divelbiss and Wen [8] proposed a method of path tracking and parking for car-like vehicles, including ones with trailers. In this approach, the environment is given, and the path is generated off line using a path space iterative algorithm. The paper is more focused on trajectory tracking for different car-trailer systems, rather than solving automatic parking problems. Miyata, Ohki, Yokouchi and Ohkita [9], [10] studied the parallel parking problem. The robot used for the implementation is an AGV. The focus of the research was to control the AGV for parallel parking using fuzzy rules and descent methods. Six transducers were used for self-localization. The system does not detect the environment for finding the parking space, and assume that the path is predefined and known.

0-7803-5180-0-5/99 $10.00 © 1999 IEEE

This paper presents an automatic parallel parking planning strategy for a car-like mobile robot, with the intention to apply the research results of robot motion planning into real-world applications. Ultrasonic sensors are used to scan the parking environment, then a path planner produces a collision-free path, which satisfies the non-holonomic constraints of the robot, for the robot to follow. Different from the approach in [7], this study has found explicit relationships for predicting all possible collisions, and defines a forbidden area, in which the robot is very likely to cause collision. The collision-free path planned outside the forbidden area provides efficient parking manoeuvres to achieve sideways displacement in backward motion as well as forward motion. The path pattern is unified, and produced in real-time once the parking space and the robot dimensions are known. The computational times for processing the path planner are recorded between 0.2 and 0.3 seconds CPU time running on a Pentium PC. This shows that the path planner needs less time than the algorithms mentioned above, and is suitable for real-time application. The strategy is implemented using a B12 mobile robot, which has been converted from a cylindrical shape to a rectangular body. The system is experimentally tested and shown capable of safe parking in tight parking spaces. The strategy presented can be used in parking aid devices, and has the potential to be integrated into automobiles.

2. MODELLING THE CAR-LIKE ROBOT

Let a robot R be a rectangular rigid object, moving around an instantaneous centre O_i. Let the robot be $2a$ long and $2b$ wide, with its wheels symmetrical about its long and short axes, as shown in Fig.1. The front wheels of the robot are steered only, as this is the case for most vehicles. A moving frame F_m is attached to R with its origin at the geometric centre of R. A reference point F lies at the middle of the back axle of the robot. In planar motions, the robot R is subject to two constraints. One of them is zero radial component of velocity. This property is expressed by Eq. (1),

$$-\frac{dx}{dt}\sin\theta+\frac{dy}{dt}\cos\theta=0 \qquad (1)$$

where x and y are the co-ordinates of the robot reference point, and θ is the orientation of the robot, referring to Fig. 1. Equation (1) is a non-integrable differential equation and hence a non-holonomic constraint.

The other constraint is the limits of the steering angle, $\alpha_{min} < \alpha < \alpha_{max}$. As the velocity v of F is greater than or equal to the product of angular speed $\frac{d\theta}{dt}$, and theminimum turning radius ρ_{min}, the second constraint can be given in inequality (2).

$$|v| \geq \left|\frac{d\theta}{dt}\right| \rho_{min} \qquad \text{i.e.}$$

Fig. 1. The model of a moving car-like robot.

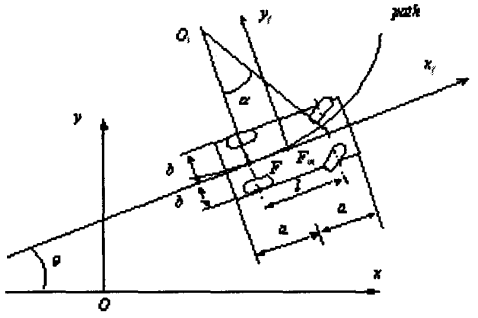

$$\left(\frac{dx}{dt}\right)^2+\left(\frac{dy}{dt}\right)^2-\rho_{min}^2\left(\frac{d\theta}{dt}\right)^2\geq 0 \qquad (2)$$

Inequality (2) is also a non-holonomic inequality constraint of the robot.

3. Automated Parking process

The automated parking process consists of three phases, which are scanning, positioning and manoeuvring to the goal position. Figure 2 illustrates a typical left-side parking process that includes the three phases. In the scanning phase, the robot moves from position 1 to position 2 to obtain information about the parking environment. In the positioning phase, the robot moves from position 2 to position 3 in preparation for a collision-free entry to the parking pace. In the manoeuvring phase, the robot moves from position 3 to the parking position 4, with forward and backward manoeuvres when necessary.

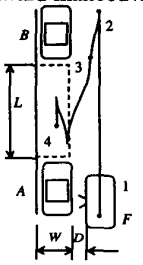

Fig. 2. Parking Example. Unit: cm. Robot: Length l=60, Width w=34, Distance D = 3.Parking space: Width W=40, Front wheel steering limit α_{limit}= 60^0, Length L=90.

3.1 Scanning Parking Space

The parking space is generally modeled as a rectangular space between two other rectangular obstacles, as shown in Fig. 2. Let the longitudinal gap between the two stationary obstacles be L, which defines the length of the parking space. Let W be the width of the parking space. The objective is to park the robot safely inside the rectangular box defined by L and W, using the least number of manoeuvres.

Ultrasonic sensors are mounted on the side of the car-like mobile robot to detect the parking environment. The sensors emit ultrasonic pulses and capture their echoes. The robot is moving along a straight-line path during scanning. Sensor data are produced reflecting distance changes beside the scanning path. The length L and the width W of the parking space are calculated after the process of sensor data, and a parking configuration, i.e. position and orientation, is produced. The normal distance D from the robot to the stationary obstacles is also found during the scanning. The wheel encoders and sensor

information are used to identify the position of the robot relative to the parking space. The obstacle locations, the start and the goal configurations of the robot are now known. This information is passed to the path planner to find a safe path.

A parking space can be different from what has been shown in Fig.2, such as it is on the right of the robot, and only one obstacle is in front or back of the parking space. This paper discusses parking to the left only. Parking to the right can be dealt with in the same way by symmetry. Once the parking system is initiated, scanning process starts immediately while the robot is moving. If obstacle *A* does not exist, the parking space length *L* is measured from the point where the robot sensors are actuated. The scanning process is designed that once the parking space is long enough for the robot to reverse directly into the parking position the robot stops and scanning ceases. So if obstacle *B* does not exists or the parking space is long enough for a direct reverse parking, the robot stops. The reverse distance for a given robot is further discussed in path planning algorithm, Section 4.2.

3.2 Positioning and Manoeuvring

In the positioning phase the robot moves from positions 2 to 3 following a path formed by two circular arcs tangentially connected to each other. The positioning phase acts as an interface between the scanning phase and the manoeuvring phase. It loosens the requirement on scanning-path direction by allowing it a small angle, say not more than 10^0, from the parking direction. It provides a safe path for the transit from position 2 to position 3, then the robot can manoeuvre to the goal.

In the manoeuvring phase, the reference point *F* of the robot is at position 3 to begin with, as indicated in Fig. 2. Position 3 is located on the same line as the bottom edge of obstacle *B*, while keeping the robot a small clearance away from the obstacle *B*. As the reference point *F* of the robot is on the back axle, position 3 ensures that the immediately followed backward move of the robot is collision-free even though the clearance is very small.

In the manoeuvring phase, the robot moves within a rectangular area, which is measured *L* by *W*. The path for the robot to follow can be a smooth curve, by following which the robot can reverse directly to the parking position. The path may also consists of a few cusps, at which the robot can follow by manoeuvring backward and forward. The details on planning a path for a given condition are discussed in the next section.

4. MOTION PLANNING ALGORITHM

4.1 Forbidden Area

Forbidden area is referred to as the area around the parking space where the appearance of the point *F* is very likely to cause collisions between the robot and obstacles. The motion planning algorithm identifies the forbidden area first, then plans a path for the robot outside the area.

In the manoeuvring phase, the robot moves into a rectangular parking area. The necessary distances the robot reference point *F* should keep away from obstacles are shown in Fig. 3. The distances h_f, h_b, w_f, and w_b are described in Eq. (3).

$$h_f = b\sin\xi + (a+\frac{l}{2})\cos\xi$$
$$h_b = b\sin\xi + (a-\frac{l}{2})\cos\xi \qquad (3)$$
$$w_f = b\cos\xi + (a+\frac{l}{2})\sin\xi$$
$$w_b = b\cos\xi + (a-\frac{l}{2})\sin\xi$$

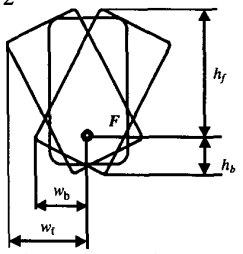

Fig. 3. Distances which the robot keeps away from obstacles.

Following authors' previous research results presented in [11]. the path in this phase is constructed by circular arcs of minimum radius ρ_{min}, tangentially linked to each other. The pattern of the path typically involves backward and forward (BF) manoeuvres as shown in Fig. 2. When the robot is close to the front or the back obstacle, its moving direction is perpendicular to the edge of the obstacle, i.e. ξ=0. Thus from Eq. (3) it can be drawn that the distances the reference point *F* should keep away from the front and back obstacles are respectively,

$$h_f = a + l/2, \quad \text{and} \quad h_b = a - l/2. \qquad (4)$$

As the robot follows circular arcs, it can be proved that it is collision-free when the robot is approaching or departing from front and back obstacle.

The width *w* the robot sweeps in parking manoeuvres depends on the orientation of the robot once its dimensions are given. The maximum width the robot requires in manoeuvring occurs when the robot is on a smooth path section, but not at a cusp of the path. Thus the distance the robot should keep away from an obstacle beside it cannot be given as a constant. However, the robot reference point *F* should keep the minimum distance w_{min} from an obstacle to avoid collisions, which is bound to happen if w_{min} is smaller. w_{min} can be achieved by letting ξ=0 in w_f and w_b in Eq.(3),

$$w_{min} = b. \qquad (5)$$

Conditions (4) and (5) are considered together to form the forbidden area. Figure 4 illustrates the forbidden area for the reference point *F*.

Avoiding forbidden area in path planning does not eliminate all collision possibilities. Collision will still

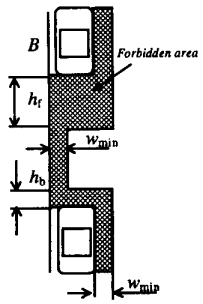

Fig. 4. Forbidden area of the robot reference point *F*.

happen if the distance between the reference point *F* and an obstacle beside the robot is less that w_f or w_b . The conditions given by w_f and w_b in (3) are taken into account in planning path for robot parking manoeuvres in section 4.3.

4.2 BF Manoeuvres

In the manoeuvring phase, a path is constructed using circular arcs of minimum radius ρ_{min} as mentioned before. This ensures that the minimum radius ρ_{min} of the circular arcs satisfies the constraint imposed by the steering limit, inequality (2). The non-holonomic constraint in Eq. (1) requires the velocity of the robot be tangent to the path. Constraint (2) also requires that no skidding occur during the rotation of the wheels.

Two arcs are used to form a path section for the robot to move backward or forward. The path section for backward motion is discussed first. A general case is shown in Fig. 5 where the robot is to move from configuration P_i to configuration P_{i+1} following an arc of circle *i* first, then an arc of circle *i*+1. A local frame is located at P_{i+1}, with *y*-axis aligning with P_{i+1} in opposite direction. $O_i(x_{oi}, y_{oi})$ and $O_{i+1}(x_{o\,i+1}, y_{o\,i+1})$ are centres of circles *i* and *i*+1. Let $w = x_i - x_{i+1}$ and $h = y_i - y_{i+1}$. If *w* is known, *h* represents the minimum distance the robot has to travel to achieve a sideways displacement *w*. It can be seen from Fig. 5. that,

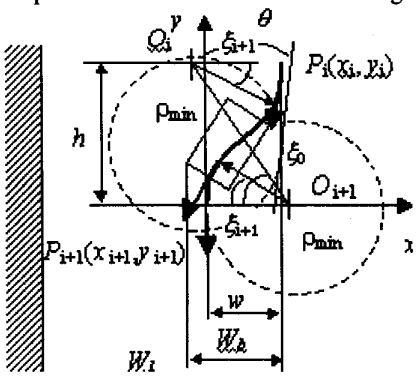

Fig. 5. A path section formed by two circular arcs.

$$w = 2\rho_{min}(1-\cos\xi_0) - \rho_{min}(1-\cos\theta)$$

$$h = 2\rho_{min}\sin\xi_0 - \rho_{min}\sin\theta$$

The relationship between *h* and *w* can be obtained by combining the equations above together.

$$h = 2\rho_{min}\sin\left[\cos^{-1}\frac{1+\cos\theta - w/\rho_{min}}{2}\right] - \rho_{min}\sin\theta;$$

$$2\rho_{min} \geq w \geq 0 \qquad (6)$$

where ρ_{min} is the minimum radius the robot can follow. ρ_{min} is determined by the steering limit α_{limit}, $\rho_{min} = l / \tan(\alpha_{limit})$.

In phase 1, Eq. (6) is used to determine the necessary distance *h* for the robot to pass by obstacle *B*, so that the robot has sufficient distance to reverse back from position 2 to position 3 to achieve sidewise displacement *w*.

An inverse expression of Eq. (6) can be written as Eq. (7), giving the maximum sidewise distance the robot can move under the non-holonomic constraints when *h* is known. Here θ is zero, because the robot is perpendicular to both front and back obstacles when it is at the cusps.

$$w = 2\rho_{min}\left[1-\cos\left(\sin^{-1}\frac{h}{2\rho_{min}}\right)\right];$$

$$2\rho_{min} \geq h \geq 0 \qquad (7)$$

4.3 BF Manoeuvre-Path Planning

The robot follows three kinds of path in its parking process. In the scanning phase, the path is a straight line. In the positioning phase, the path is a curve formed by two circular arcs of minimum radius ρ_{min}, linking configurations P_2 and P_3. As the configurations P_2 and P_3 are known, circle centres $O_2(x_{o2}, y_{o2})$ and $O_3(x_{o3}, y_{o3})$ can be found using Eq. (1). Thus, the two arcs of the path are defined. In the manoeuvring phase, the path is in a pattern of backward and forward. Specific path planning method is presented in this section.

The robot only needs two types of motions in phase three, i.e. moving backward to its left and forward to its left. The both actions require different widths, and, therefore, they are discussed separately.

The robot reverses back to its left following two circular arcs, Fig. 5. On the arc in circle *i*, the width W_b the robot sweeps is increasing as ξ_i increases until $\xi_i = \xi_0$, the linking point of the two arcs, where W_b reaches its maximum on arc *i*. On arc *i*+1 W_b is not monotonic. So it can be regarded that the maximum value of W_b happens either at the linking point, where $\xi_i = \xi_{i+1} = \xi_0$, or at a point on arc *i*+1, where the function W_b has maximum value. W_b can be generally expressed in Eq. (8),

$$W_b = \rho_{min}(1-\cos\xi_0) + (\rho_{min}+b)\cos\xi_{i+1} + (a - l/2)\sin\xi_{i+1} \qquad (8)$$

It can be found that W_b reaches its maximum at either $\xi_{i+1} = \xi_0$, or $\xi_{i+1} = \tan^{-1}\frac{a-l/2}{\rho_{min}+b}$, where $\frac{dW_b}{d\xi_{i+1}} = 0$. For a given collision-free manoeuvre distance *h*, $\xi_0 = \cos^{-1}\frac{h}{2\rho_{min}}$ is constant if the parking width is enough, referring to Fig. 5. Therefore, the maximum width W_{bmax} can be calculated by Eq. (9)

$$W_{b\max} = \rho_{\min} + \sqrt{(a-l/2)^2+b^2}\sin\left(\sin^{-1}\frac{h}{2\rho_{\min}} + \tan^{-1}\frac{b}{a-l/2}\right) \quad (9)$$

when $\xi_0 \geq \tan^{-1}\dfrac{a-l/2}{\rho_{\min}+b} \geq 0$

$$W_{b\max} = \rho_{\min}\left[1-\cos\left(\sin^{-1}\frac{h}{2\rho_{\min}}\right)\right] + \sqrt{(a-l/2)^2+(\rho_{\min}+b)^2};$$

when $\dfrac{\pi}{2} \geq \tan^{-1}\dfrac{a-l/2}{\rho_{\min}+b} \geq \xi_0$

When P_i is known, Eq. (9) is used to check whether the distance W_l between P_i and the side obstacle is sufficient for locating P_{i+1} to achieve the maximum sidewise movement with given h. If $W_l \geq W_{b\max}$, i.e. the side space is sufficient, $O_{i+1}(x_{o2}, y_{o2})$ can be determined by Eq.(10), which is derived from Eq.(1). P_{i+1} and the path section are thus defined.

$$x_{o\,i+1} = x_{oi} + 2\rho_{\min}\sin\left(\cos^{-1}\frac{h}{2\rho_{\min}}\right), \quad (10)$$

$$y_{o\,i+1} = y_{oi} - h$$

If $W_l < W_{b\max}$, the limited width W_l is used to determine the location of $O_{i+1}(x_{o\,i+1}, y_{o\,i+1})$ using Eq. (11), thus P_{i+1} and the path section are defined.

$$x_{o\,i+1} = x_{oi} + W_l$$
$$y_{o\,i+1} = y_{oi} - 2\rho_{\min}\cos\left(\sin^{-1}\frac{W_l}{2\rho_{\min}}\right) \quad (11)$$

Similarly, a path section for the robot R to move forward to its left can be defined based on P_i and the width of the parking space. Referring to Fig. 5, the maximum width $W_{f\max}$ the robot sweeps happens when the robot is moving forward along arc $i+1$. The width W_f of the space can be checked by using Eq. (12),

$$W_{b\max} = \rho_{\min} + \sqrt{(a+l/2)^2+b^2}\sin\left(\sin^{-1}\frac{h}{2\rho_{\min}} + \tan^{-1}\frac{b}{a-l/2}\right) \quad (12)$$

when $\xi_0 \geq \tan^{-1}\dfrac{a+l/2}{\rho_{\min}+b} \geq 0$

$$W_{b\max} = \rho_{\min}\left[1-\cos\left(\sin^{-1}\frac{h}{2\rho_{\min}}\right)\right] + \sqrt{(a+l/2)^2+(\rho_{\min}+b)^2};$$

when $\dfrac{\pi}{2} \geq \tan^{-1}\dfrac{a+l/2}{\rho_{\min}+b} \geq \xi_0$

$O_{i+1}(x_{o\,i+1}, y_{o\,i+1})$ can be determined by Eq. (13), when $W_l \geq W_{f\max}$;

$$x_{o\,i+1} = x_{oi} + 2\rho_{\min}\cos\left(\sin^{-1}\frac{h}{2\rho_{\min}}\right), \quad (13)$$

$$y_{o\,i+1} = y_{oi} + h$$

or by Eq. (14) when $W_{f\max} \geq W_l$.

$$x_{o\,i+1} = x_{oi} + W_l$$
$$y_{o\,i+1} = y_{oi} + 2\rho_{\min}\sin\left(\cos^{-1}\frac{W_l}{2\rho_{\min}}\right) \quad (14)$$

4.4 Speed Control

In this study it is assumed that when the robot travels along any given path segment, it is either moving at an assigned top speed v_0, if this is attainable, or accelerating/decelerating at an assigned value a_0. v_0 and a_0 are decided based on the robot specifications. The speed-time curve for the robot to travel over a path segment is as shown in Fig. 6. The longitudinal speed control scheme is formulated as below.

$$\begin{aligned} v &= a_0 t && 0 < t \leq t_1 \\ v &= v_0 && t_1 < t \leq t_2 \\ v &= v_0 - a_0 t && t_2 < t \leq T \end{aligned} \quad (15)$$

where the start time is set as 0, $t_1 = \dfrac{v_0}{a_0}$, $t_2 = \dfrac{d - v_0^2/a_0}{v_0} + t_1$, and $T=t_2+t_1$. The length of the path section d is calculated by summing up the lengths of two arcs and a straight line once the arc centres are known from eqs. (10), (11), (13), and (14).

The angular speed $\dot{\varphi}$ in steering is controlled following the same principle as for longitudinal motion, and the relationships are given as below.

$$\begin{aligned} \dot{\varphi} &= \ddot{\varphi}_0 t && 0 < t \leq \tau_1 \\ \dot{\varphi} &= \dot{\varphi}_0 && \tau_1 < t \leq \tau_2 \\ \dot{\varphi} &= \dot{\varphi}_0 - \ddot{\varphi}_0 t && \tau_2 < t \leq \Gamma \end{aligned} \quad (16)$$

where the start time is set as 0 , $\dot{\varphi}_0$ is the given top angular speed, $\ddot{\varphi}_0$ is the given angular accelaration, $\tau_1 = \dfrac{\dot{\varphi}_0}{\ddot{\varphi}_0}$, $\tau_2 = \dfrac{\delta - \dot{\varphi}_0^2/\ddot{\varphi}_0}{\dot{\varphi}_0} + \tau_1$, and $\Gamma=\tau_2+\tau_1$. The length of the arc δ can be calculated once the arc centres are known from eqs. (10), (11), (13), and (14).

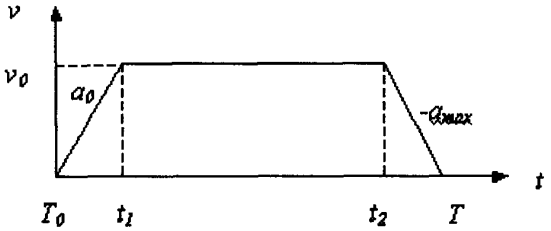

Fig. 6. Speed control scheme for longitudinal motion.

5. EXPERIMENTS

The automated parking system developed was implemented on a B12 mobile robot, which was modified into a box shape. In addition, the driving mechanism of the B12 robot was changed to keep two wheels in a fixed orientation, with only one wheel being steered. Ultrasonic sensors were mounted on the left side of the robot for detecting the environment. A notebook computer was attached to the top of the robot for running the operating program. The modified B12 robot is shown in Fig. 7.

The system control programme requires the user to set the constructional dimensions of the robot. The parking system scans the environment while the robot is moving, and drives the robot to carry out the parking actions. The programme also allows the user to inspect data files within

the control windows. Parking simulations can be run for testing, prior to parking the robot.

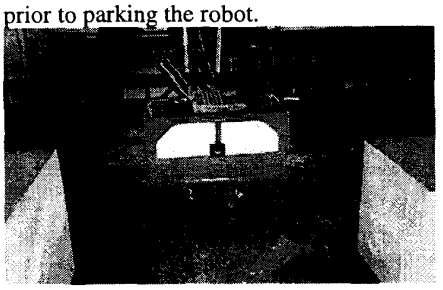

Fig. 7 Modified mobile robot and its parking environment.

The physical parameters of the car-like robot are as follows: length $2a$ = 60 cm, width $2b$ = 34 cm, front wheel steering angle $\alpha = 0^0 \sim 80^0$, back wheel steering angle $\beta = 0^0$, distance between front and back axes l = 40 cm, and distance between left and right wheels on each axle = 30 cm. The top translation speed used is v_0=90cm/s, and the acceleration is a_0=90cm/s^2. The rotation speed for steering is $\dot{\varphi}_0 = 130^0$/s, and the rotation acceleration is $\ddot{\varphi}_0 = 130^0/s^2$.

Many different parking situations were successfully tested. Figure 8 shows a typical parking example. When the front wheel steering angle is set to $\alpha=50^0$, and the length of the parking space is set to L=130cm, a path consisting two BF manoeuvres is produced, taking 0.24 seconds. When the length of the parking space is set to L=100 cm and L=130 cm, paths produced consist of three and one BF manoeuvres respectively The times for producing the two paths are 0.26 and 0.23 seconds CPU time. The experimental results show that the parking manoeuvres are sensitive to the parking space length, which is as expected.

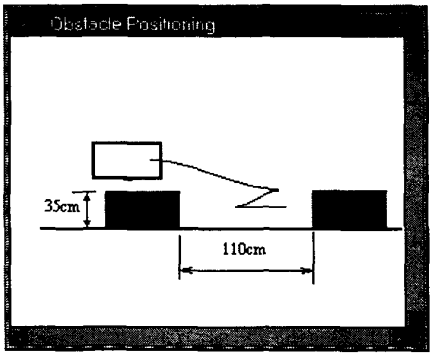

Fig. 8 A parking manoevure example .

6. CONCLUSIONS

The paper presents the study of the parallel parking problem for a car-like mobile robot, aiming at developing an automated parking aid device, then integrating the system into vehicles. The parking system, guided by ultrasonic sensors, works in three phases, scanning, positioning, and manoeuvring. Parking environment is scanned using ultrasonic sensors once the system is initiated. The scanning data are processed to identify the parking space and parking position of the robot. Then the robot moves to the edge of the parking space, followed by unified collision-free manoeuvres to reach the goal position.

Characteristics of a car-like robot have been analyzed, and an algorithm has been developed for producing a real-time collision-free path which leads to efficient parking manoeuvres. The path is planned based on mathematical models, varying with the dimensions of the parking space. Non-holonomic constraints imposed on the robot have been met in the path. The robot may reverse into its parking position if the space is sufficient, or moves backward-forward to reach it if the space it small. Warning will be issued and no action is taken if the space is too small to park the robot.

The novel contributions of the paper include a robot motion planning algorithm for parking in small parking spaces, its related mathematical descriptions of models and control equations, experimental implementation, and system integration.

The system is implemented on a B12 mobile robot. The body of the robot has been reshaped from cylindrical to rectangular shape. Ultrasonic sensors are mounted on the robot for detecting the parking space and obstacles. A control programme in the form of a graphical user interface has been developed for the user to operate the system with ease. The system has been extensively tested and shown to be capable of automatic parking in small parking spaces.

References:

[1] G. Lafferriere and H.J. Sussmann, "Motion planning for controllable systems without drift: a preliminary report", Technical Report SYCON-90-04, Rutgers University, June, 1990.

[2] R.M. Murray and S.S.Sastry, "Steering nonholonomic systems using sinuoids", 29th C.D.C., Honolulu, Dec. 1990.

[3] H.J. Sussmann and W. Lui, "Limits of highly oscillatory controls and the approximation of general paths by admissible trajectories", Report SYCON-91-02, Rutgers University, 1991.

[4] P. Jacobs, J. P. Laumond and M. Taix, "Efficient motion planners for nonholonomic mobile robots", *Proceedings of 1991 IEEE IROS*, Osaka, November 1991.

[5] Zexiang Li and J. F. Canny, *Nonholonomic Motion Planning*, Kluwer Academic Publishers, 1993

[6] J. P. Laumond, Paul E. Jacobs, Michel Taix, and Richard M. Murry, " A motion planner for nonholonomic mobile robots", IEEE Trans. on robotics and automation, Vol. 10, No. 5, October 1994

[7] I.E. Paromtchik and C. Laugier, "Autonomous Parallel Parking of a Nonholonomic Vehicle", IEEE Intelligent Vehicles Symposium, NJ, USA, pp13-18, 1996

[8] A.W. Divelbiss and J.T. Wen, "Trajectory tracking control of a car-trailer system", IEEE Transactions on Control systems technology, Vol.5, No.3, pp.269-278, 1997.

[9] H.Miyata, M. Ohki, Y.Yokouchi and M.Ohkita, "Control of the autonomous mobile robot Dream-1 for a parallel parking", Math & Comp. in Simulation, Vol. 41, No 1-2, pp129-138. 1996.

[10] H.Miyata, M. Ohki and M.Ohkita, "Self-tuning of fuzzy-reasoning by the steepest descent method and its application to a parallel parking", IEICE Transactions on Information and Systems, Vol. E79D, No. 5, pp.561-569, 1996.

[11] K. Jiang, L.D. Seneviratne and S.W.E. Earles, "Motion planning with reversal manoeuvres for a non-holonomic constrained robot", Journal of Engg. Manufacture, IMechI, Vol 210, 1996, pp487-497